A Modern Method for Analyzing Related Substances of Cabotegravir and Rilpivirine Using RP-HPLC, along with the Characterization of their Degradation Products Via LCMS

Sailaja Ommi, Krishnaveni Gudela, Swathi Kongala

Department of Chemistry, K.B.N. College, Vijayawada, Andhra Pradesh, India

Abstract

Introduction: The estimation, separation, and validation of Cabotegravir and Rilpivirine along with their impurities were performed using the RP-HPLC technique. **Materials and Methods:** Cabotegravir, Rilpivirine, and their respective impurities were separated on an Inertsil ODS column (150 × 4.6 mm, 3.5 μ) using a mobile phase consisting of 5 mM Ammonium Formate and acetonitrile at a flow rate of 1 mL/min at room temperature. The PDA detector from a Waters HPLC e-2695 quaternary pump was used with a wavelength of 231 nm. The linearity was investigated for 17 min with injection concentrations of 75–450 μg/mL of Rilpivirine, 50–300 μg/mL of Cabotegravir, and 1.25–7.5 μg/mL of each impurity of Cabotegravir and Rilpivirine. The validity of the proposed method was verified using the International Conference on Harmonization (ICH) guidelines. **Results and Discussion:** The results of method validation including specificity, linearity, accuracy, ruggedness, and robustness were within the permissible range. **Conclusion:** The HPLC-MS technique successfully validated the chemical structures of the degradation products of Cabotegravir and Rilpivirine, and stress studies were carried out in compliance with ICH Q2 (R1) guidelines.

Key words: Cabotegravir, HPLC, related impurities, rilpivirine, validation

INTRODUCTION

Cabotegravir, also known by the brand name Vocabria, is an antiretroviral[1,2] drug that is effective against HIV/AIDS.[3,4] It is marketed as Cabenuva, an injectable combination drug, and is also sold separately as tablets and intramuscular injections.[5] Cabotegravir is an integrase inhibitor with a carbamoyl pyridone structure similar to that of dolutegravir. It is approved for use in combination with rilpivirine to treat people with HIV-1.[6,7] This combination injection is intended for adults who have undetectable HIV levels in their blood and whose virus has not yet developed resistance to non-nucleoside reverse transcriptase inhibitors (NNRTIs)[8] and integrase strand transfer inhibitors. These drugs are the first antiretroviral treatments available in an extended-release injectable form. The most common adverse effects of rilpivirine injection treatment are pain and swelling at the injection site, which can occur in up to 84% of patients. Headache (up to 12%) and fever (up to 10%) are also common side effects. The frequency of side effects, including headache and feeling overheated, decreased somewhat for the pill form of the medication. Less common adverse effects (<10%) for both formulations include depressive disorders,[9,10] sleeplessness,[11,12] and rashes.[13]

Rilpivirine, marketed as Edurant and Rekambys by Tibotec, is an antiretroviral drug used to treat HIV/AIDS.[14] It is a second-generation NNRTI that is more effective and has a longer half-life than first-generation NNRTIs like efavirenz,[15] and also has fewer adverse effects. However, it should not be taken with medications like carbamazepine,[16,17] phenytoin,[18] rifampicin, or St. John's wort, which increase the liver enzyme

Address for correspondence:
Krishnaveni Gudela, Department of Chemistry,
K.B.N. College, Vijayawada, Andhra Pradesh, India.
E-mail: gudelakrishnaveni@gmail.com

CYP3A4.[18,19] These medicines can hasten rilpivirine's breakdown, leading to lower plasma concentrations and potentially reduced efficacy and resistance. Some of these medications also stimulate the enzyme UGT1A1[20,21] and lower plasma concentrations of cabotegravir, further reducing the combination treatment's efficacy. Proton pump inhibitors are also contraindicated when used in combination with rilpivirine since they raise stomach pH and prevent adequate absorption from the intestines.[22,23] The injectable formulation can cause pain and swelling at the injection spot (in up to 84% of patients), headache (in up to 12%), and fever (in up to 10%). Mental health issues such as depression, sleeplessness, and skin rashes all fall under the 10% category. These adverse effects occurred during HIV treatment regimens that used rilpivirine in conjunction with other medications. Therefore, we developed an RP-HPLC technique to determine Cabotegravir and Rilpivirine concentrations and identify and remove associated contaminants. Figure 1 shows the structures for Cabotegravir, Rilpivirine, and their related substances.

MATERIALS AND METHODS

Chemicals

We obtained our HPLC-grade acetonitrile and ammonium formate from Merck India Ltd in Mumbai, India, and our HPLC-grade water from Milli-Q. Candila Health Care Ltd. of Ahmedabad, India, provided us with Cabotegravir, Rilpivirine, their related impurities, and samples.

Instrumentation

We used the Waters Alliance e-2695 HPLC system with a quaternary pump and a PDA scanner equipped with the Empower version 2.0 program.

HPLC-MS

During the forced degradation investigation, we positioned a splitter in front of the ESI source, allowing only 35% of the eluent to enter the HPLC system. To perform MS scans of Cabotegravir and Rilpivirine in positive ESI mode, we used a fragmentor voltage of 80V, a capillary voltage of 3000V, a skimmer voltage of 60V, nitrogen as the drying and nebulizing gas at 45psi, and highly filtered nitrogen gas as the collision gas.

Preparation of mobile phase-A

Ammonium formate (6.3 g) was filtered using 0.45 µ filter paper after being dissolved in 1 L of HPLC-grade water.

Mobile phase-B

Acetonitrile.

Optimization of mobile phase

The development of the procedure relied on the use of buffers and mobile phases, but all trials resulted in improper peak separation. Finally, the suggested approach was able to resolve all peaks, and all necessary requirements for applicability were met.

Gradient program: Gradient program is shown in Table 1.

There has been an increased interest in developing a method for determining Cabotegravir, Rilpivirine, and their associated impurities using HPLC due to the absence of published techniques.
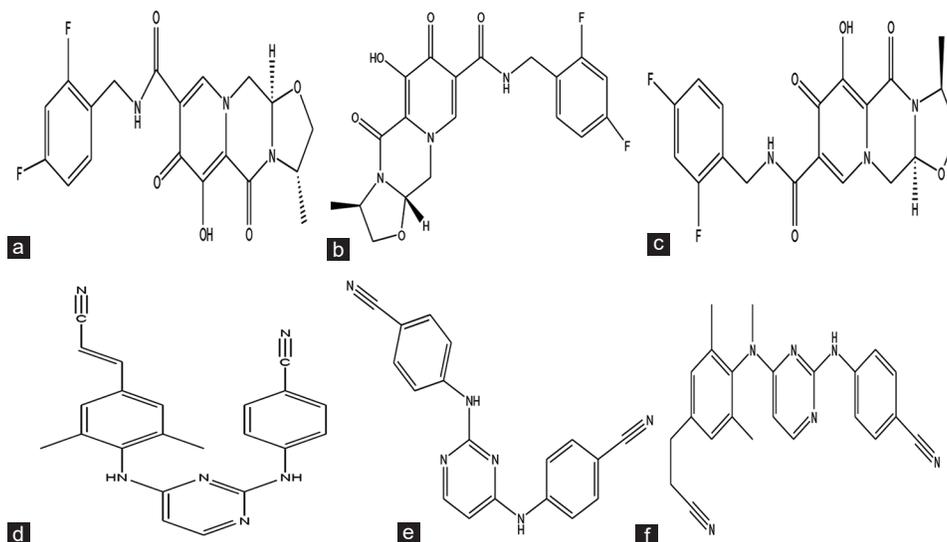
Figure 1: Chemical representation of (a) Cabotegravir, (b) CBG Imp-1, (c) CBG Imp-2, (d) Rilpivirine, (e) RLP Imp-1, and (f) RLP Imp-2

Chromatographic conditions

At a flow rate of 1 mL/min, an inertsil ODS (150 × 4.6 mm, 3.5 μ) column was used for reverse-phase HPLC analysis operating in gradient elution mode with acetonitrile and ammonium formate as the mobile phase.

Diluent

Mobile phase was used as diluent.

Standard stock solution

Rilpivirine (30 mg) and Cabotegravir (20 mg) should be accurately weighed and then transferred to a 10 mL volumetric flask. Add 7 mL of diluent and sonicate for 10 min to dissolve the contents.

Sample stock solution

1 ml of sample (containing 200 mgs of Cabotegravir and 300 mgs of rilpivirine) should be diluted to 100 ml in a volumetric flask.

Impurity stock solution

Cabotegravir imp-1 (5 mg), Cabotegravir imp-2 (5 mg), Rilpivirine imp-1 (5 mg), and Rilpivirine imp-2 (5 mg) should be weighed and transferred to a 100 mL volumetric flask. Add 70 mL of diluent and sonicate for 10 min to dissolve the contents.

Spiked standard solution

5 mL of impurity stock solution to standard and 5 mL of standard stock were added to a volumetric flask of 50 mL syringe filter with a 0.45 micron pore size was used to filter the solution.

Spiked sample solution

5 mL of impurity stock solution and 5 mL of stock were added to a volumetric flask of 50 mL. Syringe filter with a 0.45 micron pore size was used to filter the solution.

Table 1: Gradient program		
Time (min)	Mobile phase-A	Mobile phase-B
0	80	20
5	50	50
7	20	80
10	20	80
12	80	20
17	80	20

RESULTS AND DISCUSSION

The main analytical challenge encountered during the development of a new technique was the separation of the active pharmaceutical components. The chromatographic conditions were adjusted to achieve optimal performance.

Method validation

The optimized RP-HPLC validation technique meets or exceeds the requirements set forth by the International conference on harmonization (ICH) guidelines in terms of system suitability, linearity, accuracy, precision, and robustness.

System suitability

System suitability testing was performed by injecting standard solutions spiked with 200 μg/mL Cabotegravir, 300 μg/mL Rilpivirine, and 5 μg/mL of each of Cabotegravir imp-1 and Cabotegravir imp-2, as well as Rilpivirine imp-1 and Rilpivirine imp-2 in six separate injections. The results, presented in Table 2, demonstrate that the machine's fitness parameter complies with the ICH guidelines. Figure 2 shows the standard chromatogram.

Specificity

To test for contamination, three different data sets were analyzed – one for the placebo, one for the sample, and one for the reference standard. The results indicated that the active ingredients and associated compounds were successfully separated from the placebo and its excipients. Figure 3 shows a blank chromatogram.

Linearity

Linearity was assessed by comparing peak area to corresponding concentration in a calibration curve. The curve demonstrated that the concentrations of Rilpivirine,

Table 2: Results of system precision			
System suitability parameter	Acceptance criteria	Cabotegravir	Rilpivirine
USP plate count	NLT 2000	19845	9037
USP tailing	NMT 2.0	1.12	1.01
USP Resolution	NLT 2.0	-	2.86
% RSD	NMT 2.0	0.75	0.86
Retention time	NLT 2.0	6.941	4.117

RSD: Relative standard deviation
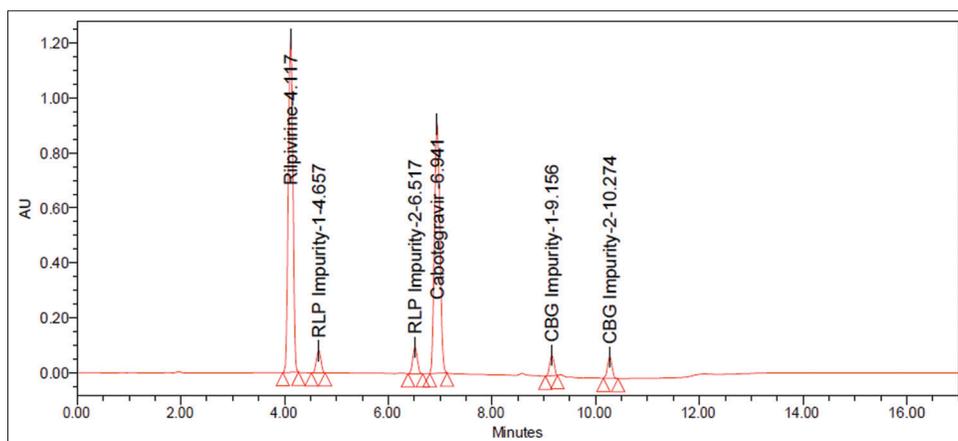
Figure 2: Standard chromatogram
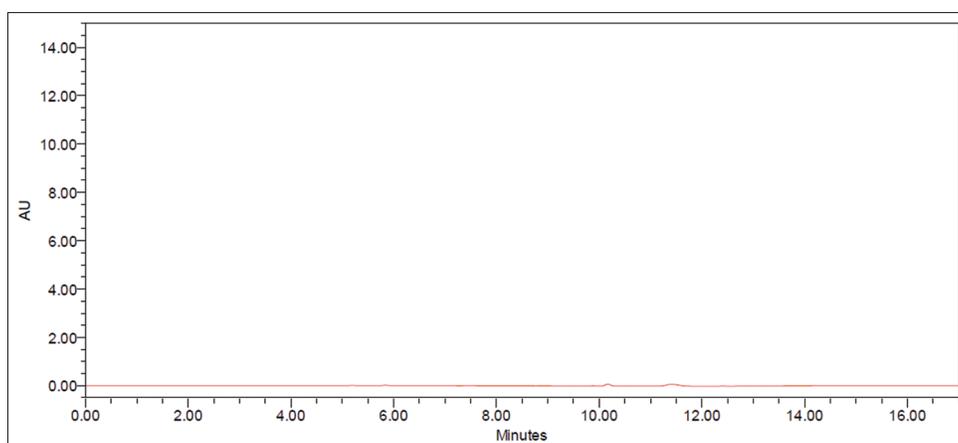
Figure 3: Blank chromatogram

Cabotegravir, and their related impurities linearly ranged from 75 to 450 µg/mL, 50 to 300 µg/mL, and 1.25 to 7.5 µg/mL, respectively. The calibration curves' regression equations were Y = 226892.84x+181471 (R2 = 0.99929) for Rilpivirine, Y = 96034.42x+3966.40 (R2 = 0.9998) for Rilpivirine Impurity-1, Y = 120073.94x+6154.63 (R2 = 0.9999) for Rilpivirine Impurity-2, Y = 336069.78x+313475.35 (R2 = 0.99985) for Cabotegravir, Y = 85901.15x+597.08 (R2 = 0.9999) for Cabotegravir Impurity-1, and Y = 93542.22x+313475.35 (R2 = 0.99983) for Cabotegravir Impurity-2, respectively. The linearity results are presented in Table 3 and the calibration plots are shown in Figure 4.

Accuracy

To verify the accuracy of the method, we conducted a study to determine the recovery at three different levels (50%, 100%, and 150%). Active pharmaceutical ingredients were prepared with concentrations of 150, 300, and 450 µg/mL for Rilpivirine, 100, 200, and 300 µg/mL for Cabotegravir, and 2.5, 5, and 7.5 µg/mL for Rilpivirine imp-1, Rilpivirine imp-2, Cabotegravir imp-1, and Cabotegravir imp-2. The test solution was injected 3 times at each spike level. The relative

standard deviation (RSD) values were <2%, and the recovery rates were close to 100%. The mean, RSD, and percentage of recovery were calculated, and the recovery values fell within the acceptable range. Table 4 presents the results for accuracy.

Precision

The precision of an analysis is determined by the closeness of the individual measurements in a sequence taken from several samples of the same homogenous mixture. In this study, six different determinations of Rilpivirine, Cabotegravir, and their associated compounds were used to determine the accuracy of the drug processes.

Intraday precision

On the same day, six identical solutions containing Rilpivirine, Cabotegravir, and related compounds were analyzed. The mean, standard deviation, and RSD of the peak areas were calculated. The results for the method's precision are presented in Table 5 and Figure 5 shows a chromatogram of the sample.

Linearity	Rilpivirine		Imp-1		Imp-2	
	Conc. (µg/mL)	Area	Conc. (µg/mL)	Area	Conc. (µg/mL)	Area
Linearity-1	75.00	17065146	1.25	120320	1.25	155274
Linearity-2	150.00	34987545	2.50	242621	2.50	305402
Linearity-3	225.00	51720561	3.75	360218	3.75	456528
Linearity-4	300.00	70502364	5.00	482145	5.00	602547
Linearity-5	375.00	85874157	6.25	608651	6.25	758248
Linearity-6	450.00	99889585	7.50	724156	7.50	907814
Slope	226892.84		96034.42		120073.94	
Intercept	181471.00		3966.40		6154.63	
CC	0.99929		0.99981		0.99991	
Linearity-1	50.00	17745124	1.25	106235	1.25	120414
Linearity-2	100.00	34120459	2.50	218564	2.50	238564
Linearity-3	150.00	51653285	3.75	322415	3.75	350213
Linearity-4	200.00	66523148	5.00	435261	5.00	463251
Linearity-5	250.00	84025635	6.25	533620	6.25	595412
Linearity-6	300.00	101452471	7.50	645718	7.50	699321
Slope	336069.78		85901.15		93542.22	
Intercept	313475.35		1101.15		1597.08	
CC	0.99985		0.99993		0.99983	

Table 3: Linearity results of Rilpivirine and its impurities A

Table 4: Results of accuracy

S. No.	% Level	Rilpivirine % Recovery	Cabotegravir % Recovery
1	50	100.18	100.57
2	100	100.86	100.49
3	150	100.10	100.62
Mean		100.38	100.56
Std Dev		0.418	0.066

mean±SD (*n*=3)

Inter-day precision

Inter-day precision was evaluated by analyzing six replicate samples of Rilpivirine, Cabotegravir, and their related compounds on separate days. The peak areas were determined and the mean, standard deviation, and RSD were calculated. The results are presented in Table 6.

LOD and LOQ

The calibration curve method was used to establish the LOD and LOQ. By injecting progressively decreasing concentrations of the standard solution, the LOD and LOQ of the chemical were determined using the formulated RP-HPLC technique. In Table 7, we see the LOD and LOQ concentrations of Rilpivirine, Cabotegravir, and their related chemicals, as well as their s/n values. Figure 6 shows LOD and LOQ chromatograms. This procedure has been shown reliable in accordance with ICH regulations.

Robustness

The experimental setup was designed to assess the ability of the system to perform consistently across a wide range of situations, even when variables such as flow rate and mobile phase organic percentage were deliberately altered. The results of the robustness analysis for Rilpivirine, Cabotegravir, and their associated impurities are presented in Table 8, indicating that all values were within the allowable range.

Degradation studies

Attempts were made to induce partial breakdown of the chemical by subjecting Rilpivirine, Cabotegravir and similar compounds to various forced degradation conditions. Experiments with forced degradation have proven; the approach is suitable for degradation materials. The investigations also detail the range of temperatures and pressures under which the medicine becomes unstable, allowing for preventative measures to be adopted during formulation. HPLC-MS allowed for the detection and characterization of seven distinct DPs (DP1–DP7). In many cases, the research helped to prevent medication instability by providing data on the conditions under which it became
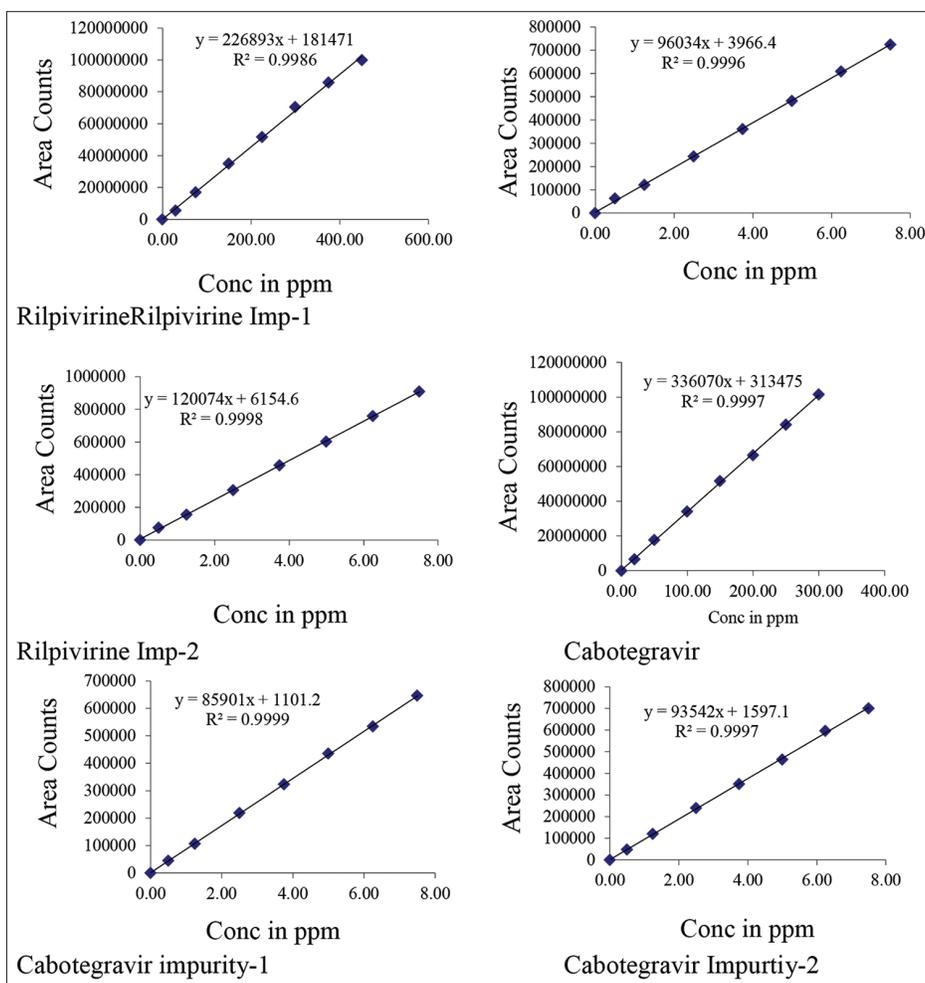
**Figure 4:** Calibration plots of Cabotegravir, Rilpivirine and their related impurities
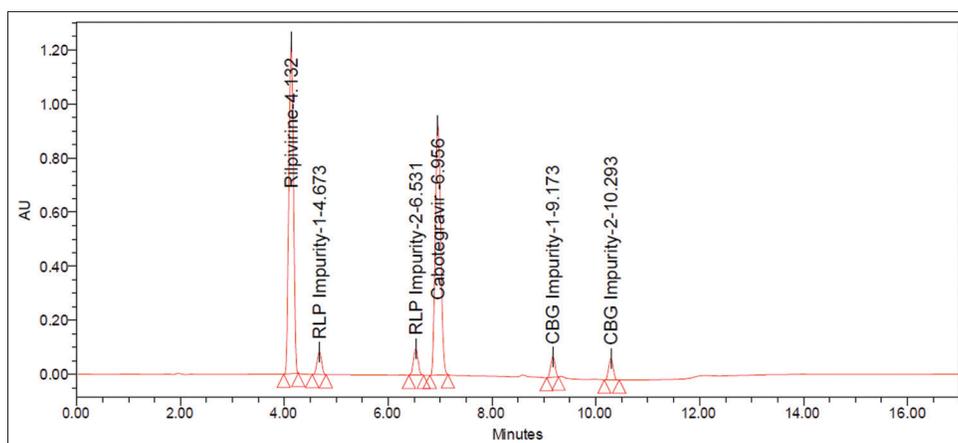
Figure 5: Chromatogram of sample

unstable. The degradation data for Cabotegravir and Rilpivirine are shown in Table 9.

Acid degradation

Rilpivirine and Cabotegravir were subjected to acid degradation in 1N HCl, with degradation rates of 13.3% and

11.4%, respectively, resulting in the formation of DP1 and DP5, respectively.

Alkali degradation

Using 1N NaOH for alkali degradation, we found that 12.1% of the Rilpivirine and 10.5% of the Cabotegravir

Table 5: Intraday precision results of (A) rilpivirine and (B) cabotegravir

(A)

Sample No.	% of related substances		
	Spiked impurities	Total impurities	% Purity (100-Total impurities)
1	1.26	0.24	99.76
2	1.23	0.27	99.73
3	1.25	0.25	99.75
4	1.28	0.22	99.78
5	1.27	0.23	99.77
6	1.24	0.26	99.74
Average	1.26	0.25	99.76
% RSD	1.49	7.64	0.02

(B)

Sample No.	Spiked impurities	Total impurities	% Purity (100-Total impurities)
1	2.46	0.54	99.46
2	2.43	0.57	99.43
3	2.45	0.55	99.45
4	2.49	0.51	99.49
5	2.51	0.49	99.51
6	2.48	0.52	99.48
Average	2.47	0.53	99.47
% RSD	1.17	5.47	0.03

mean±SD (*n*=6)

Table 6: Inter-day precision results of (A) Rilpivirine and (B) Cabotegravir

(A)

Sample No.	% of related substances		
	Spiked impurities	Total impurities	% Purity (100-Total impurities)
1	1.27	0.23	99.77
2	1.24	0.26	99.74
3	1.28	0.22	99.78
4	1.25	0.25	99.75
5	1.27	0.23	99.77
6	1.25	0.25	99.75
Average	1.26	0.25	99.76
% RSD	1.23	7.64	0.016

(B)

Sample No.	Spiked impurities	Total impurities	% Purity (100-Total impurities)
1	2.46	0.52	99.48
2	2.43	0.55	99.45
3	2.45	0.54	99.46
4	2.49	0.56	99.44
5	2.51	0.55	99.45
6	2.48	0.54	99.46
Average	2.47	0.54	99.46
% RSD	1.17	2.51	0.01

Table 7: LOD and LOQ results

Name	LOD Conc. (µg/mL)	S/N	LOQ Conc. (µg/mL)	S/N
Rilpivirine	0.9	3	3	10
Imp-1	0.015	3	0.05	10
Imp-2	0.015	3	0.05	10
Cabotegravir	0.6	3	2	10
Imp-1	0.015	3	0.05	10
Imp-2	0.015	3	0.05	10

Table 8: Robustness results of Rilpivirine and Cabotegravir

Parameter name	Rilpivirine	Cabotegravir
	% RSD	
Flow rate (0.9 mL/min)	0.89	0.47
Flow rate (1.1 mL/min)	0.56	1.05
Org plus (+10%)	0.84	1.02
Org minus (−10%)	0.34	0.27

Table 9: Forced degradation results of Rilpivirine and Cabotegravir

Degradation condition	Rilpivirine	Cabotegravir
	% purity	
Acid deg	13.3	11.4
Alkali deg	12.1	10.5
Peroxide deg	14.7	12.3
Reduction deg	10.4	5.3
Thermal deg	8.9	4.1
Photo deg	3.5	2.8
Hydrolysis deg	2.7	1.9

were degraded, with DP2 and DP6 being generated as byproducts.

Peroxide degradation

The use of 30% peroxide resulted in the breakdown of Rilpivirine (14.7%) and Cabotegravir (12.3%) with the formation of DP3 and DP7 as byproducts.

Reduction degradation

Using a 30% sodium bisulfate solution, we observed a degradation of 10.4% Rilpivirine and 5.3% Cabotegravir, leading to the formation of the DP4 degradation product.

Thermal degradation

At 105°C, 8.9% of Rilpivirine and 4.1% of Cabotegravir degraded without producing any detectable degradation products.
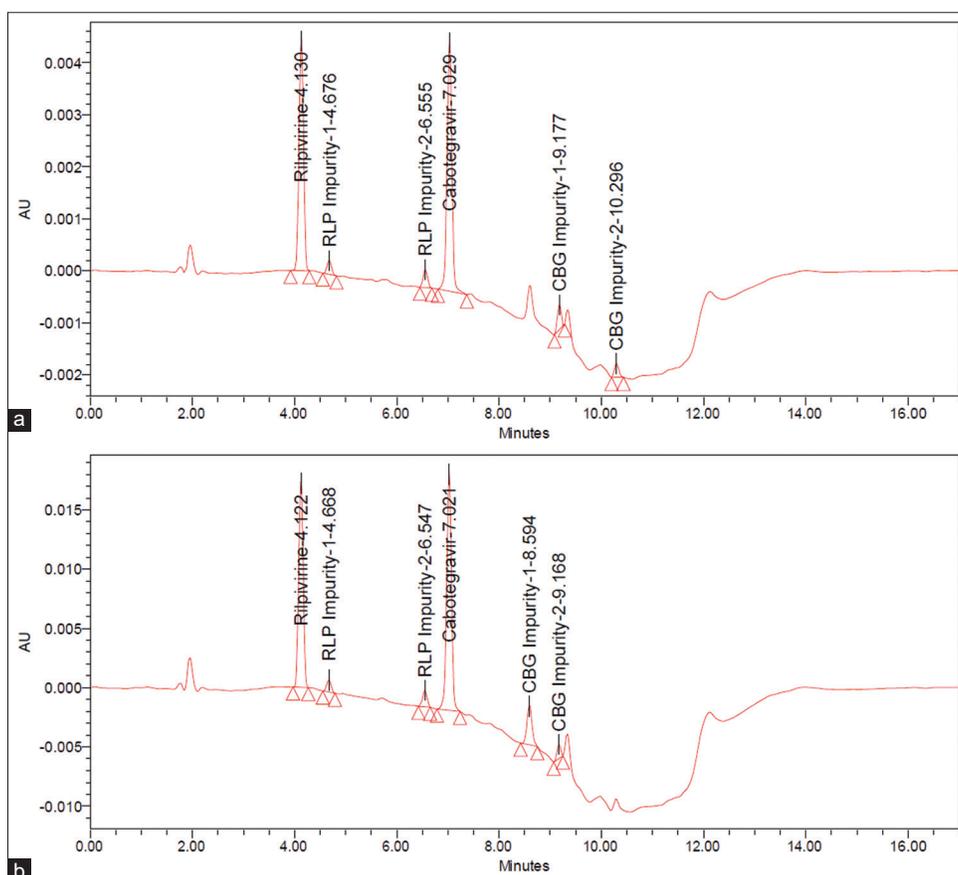
Figure 6: Chromatogram of (a) LOD and (b) LOQ

Photodegradation

Photodegradation under UV light resulted in 3.5% Rilpivirine degradation and 2.8% Cabotegravir degradation, with no degradation products being generated.

Hydrolysis degradation

When utilizing HPLC water for hydrolysis degradation, 2.7% Rilpivirine and 1.9% Cabotegravir degradation was detected, with no degradation products being produced.

CONCLUSION

The proposed technique demonstrated satisfactory results in the simultaneous identification and quantification of Rilpivirine, Cabotegravir, and their impurities. With a run time of 17 min, the method proved to be highly efficient and compliant with the amended SST criteria of USP. An Inertsil ODS column was used in the experiment, which was found to enhance the elution of analytes with high resolution, plate count, and tailing. The approach was found to be straightforward, precise, accurate, linear, robust, and quick, making it suitable for routine analysis of Rilpivirine and Cabotegravir in combination dose form. Thenon-interference

of the estimate was indicated by the fact that the sample recovery agreed well with label claims. Overall, this method is convenient and easy to use.

Collision induced dissociation of Cabotegravir and Rilpivirine

Scheme 1:Rilpivirine DP1's fragmentation process is shown in Scheme 1, and the ESI spectra revealed the presence of a particularly abundant [M+H]+ ion at m/z-423 under acid degeneration. Abundant product ions at m/z-272 (because to the loss of $C_7H_6ClN_2$), m/z-172 (due to the loss of $C_3H_3ClN_2$ from m/z 272), and m/z-53 (due to the loss of $C_8H_{11}N$ from m/z 172) were seen in the MS/MS spectra of DP1. Accurate mass measurements and MS/MS investigations both provide support to the suggested framework. Both the mass fragmentation methods and the MS spectra degradation product are shown in Figures 7 and 8.

Scheme 2: Rilpivirine DP2's fragmentation process is shown in Scheme 2, and under alkali degradaton conditions, a more intense [M+H] ion of m/z-287 was seen in the MS/MS spectrum. The m/z -172 (loss of $C_3H_4ClN_3$) and m/z -53 ($C_8H_{11}N$ lost from m/z 172) product ion abundances were quite prominent in the spectrum. The suggested methodology was validated by MS/MS tests and accurate mass calculations. The by-product of mass

fragmentation techniques and mass spectrometry is shown in Figures 9 and 10, respectively.

Scheme 3: The fragmentation process of Rilpivirine DP3 of m/z 404, which was observed under peroxide degradation condition, is shown in Scheme 3. A large number of product ions can be seen in the MS spectrum at m/z-272 (because to the loss of $C_7H_6N_2O$), m/z-172 (due

to the loss of $C_3H_3ClN_2$ from m/z 272), and m/z-53 (due to the loss of $C_8H_{11}N$ from m/z 172). The suggested technique was validated by MS/MS measurements and accurate mass assessments. Mass fragmentation schemes and the degraded MS spectra are shown in Figures 11 and 12, respectively.

Scheme 4: The fragmentation process for m/z-468 Rilpivirine DP4 observed under a reduced degradation was shown in Scheme 4. Abundant product ions can be seen in the spectrum at m/z-367 (due to the loss of C_7H_5N), m/z-272 (due to the
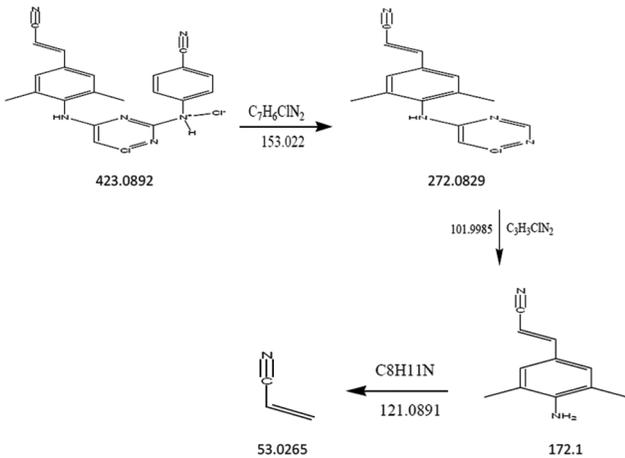
Figure 7: Mass fragmentation of scheme 1
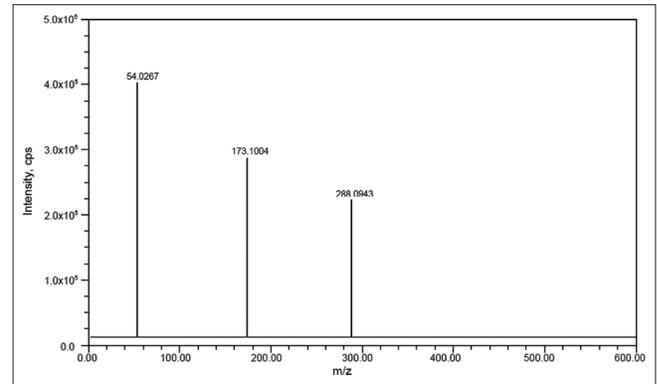
Figure 10: Mass spectra of DP2
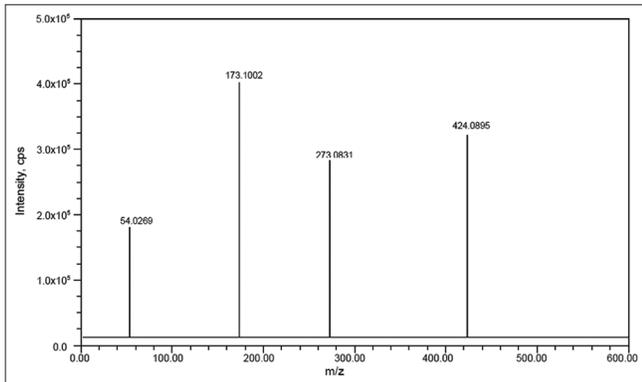
Figure 8: Mass spectra of DP1
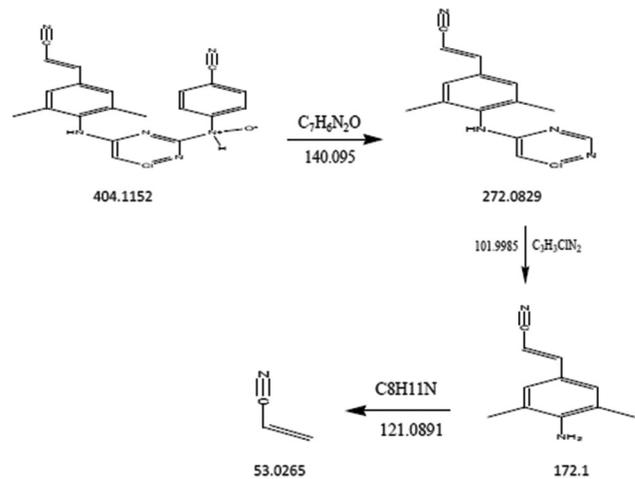
Figure 11: Mass fragmentation of scheme 3
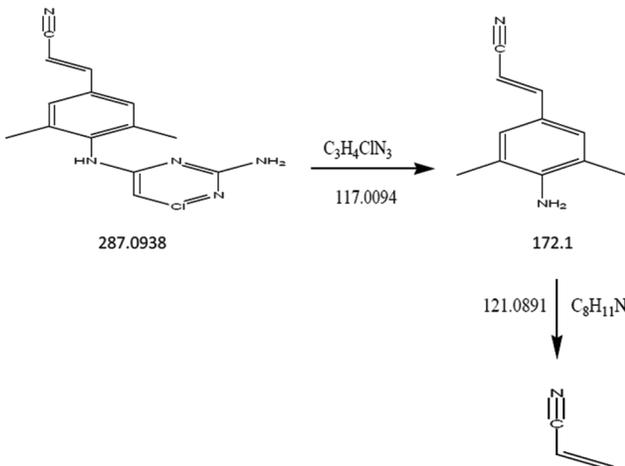
Figure 9: Mass fragmentation of scheme 2
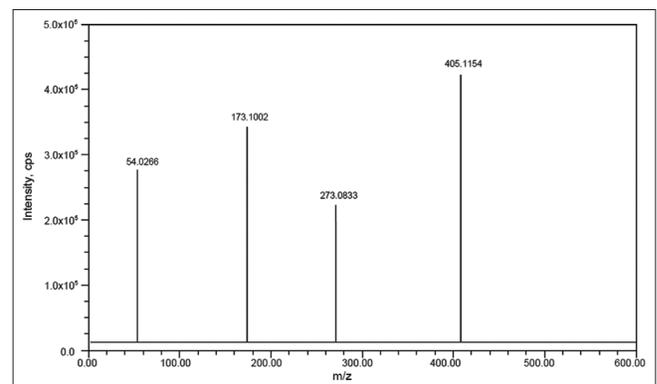
Figure 12: Mass spectra of DP3

loss of H_3NSO_3 from m/z 367), m/z-172 (due to the loss of $C_3H_3ClN_2$ from m/z 272) and m/z-53 (due to the loss of $C_8H_{11}N$ from m/z 172). The suggested methodology was validated by MS/MS tests and accurate mass calculations. Mass fragmentation techniques and the resulting MS spectra degradation are shown in Figures 13 and 14, respectively.

Scheme 5: Cabotegravir DP5 m/z-440 fragmentation was observed during acid degradation, and the resulting fragmentation process is shown in Scheme 5. Abundant product ions can be seen in the spectrum at m/z -328 (due to the loss of $C_6H_4F_2$), m/z -236 (due to the loss of C_2H_5ClNO from m/z 328), and m/z -116 (due to the loss of $C_6H_6O_3$ from m/z 236). The suggested approach has been verified by MS/MS tests and accurate mass assessments. Mass fragmentation schemes and the degraded MS spectra are shown in Figures 15 and 16, respectively.

Scheme 6: Cabotegravir DP6 fragmentation at m/z-302 was observed in an alkaline degradation environment and this is shown in Scheme 6. Abundant product ions may be seen at m/z-184 (due to the loss of $C_4H_3NaO_3$) and m/z-101 in the spectrum (loss of $C_3H_5NO_2$). The suggested approach has been verified by MS/MS tests and accurate mass assessments. Mass fragmentation schemes and the resulting MS spectra deterioration are shown in Figures 17 and 18, respectively.


Figure 13: Mass fragmentation of scheme 4
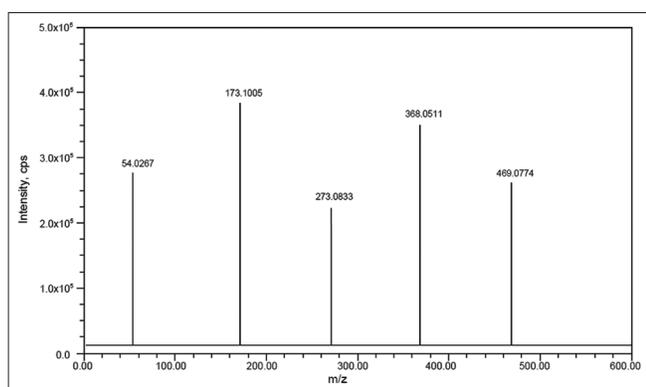
Figure 14: Mass spectra of DP4
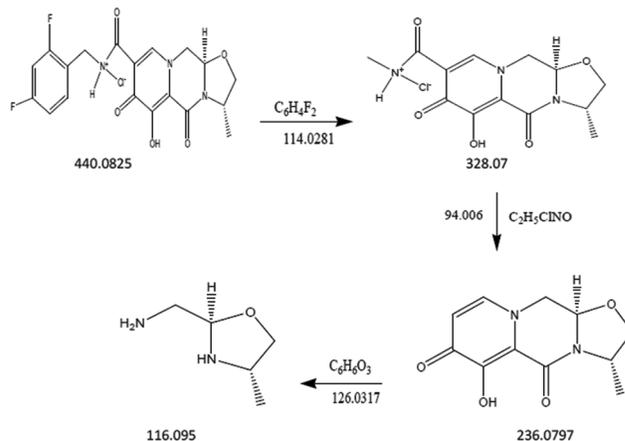
Figure 15: Mass fragmentation of scheme 5
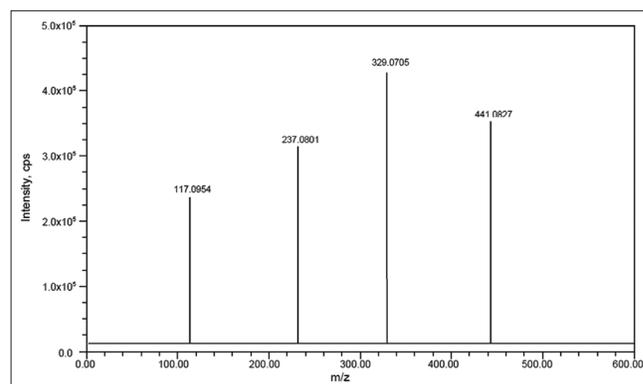

Figure 16: Mass spectra of DP5
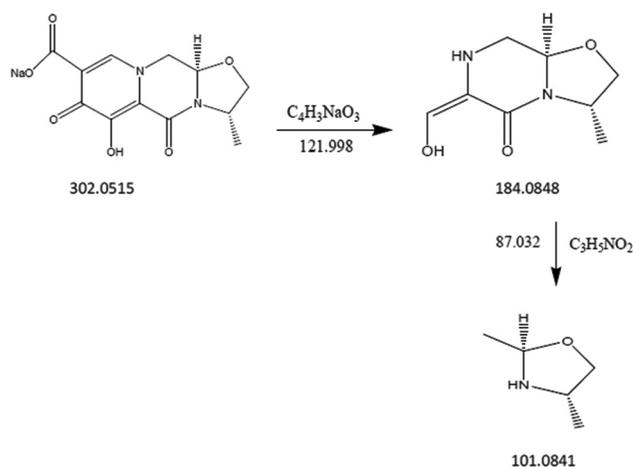
Figure 17: Mass fragmentation of scheme 6

Scheme 7: Cabotegravir degradation product 7 of m/z-421 was observed under peroxide degradation conditions, and its fragmentation process is shown in Scheme 7. The m/z-309 ($C_6H_4F_2$), m/z-236 ($C_2H_5NO_2$), and m/z-87 (C_7H_7NO) product ions are quite numerous in the spectrum. The suggested approach has been verified by MS/MS tests and accurate mass assessments. The decomposition result of MS spectra and mass spectral fragmentation techniques is shown in Figures 19 and 20, respectively.
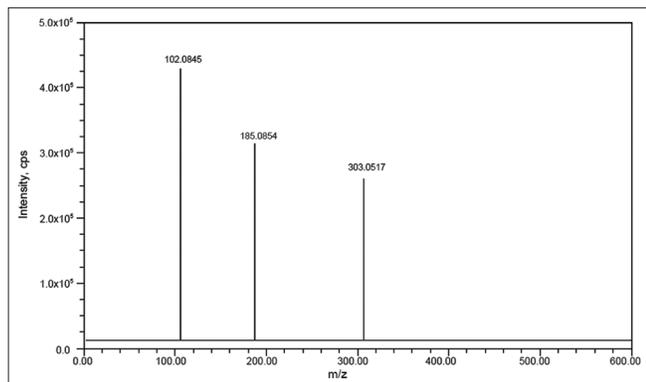

**Figure 18:** Mass spectra of DP6
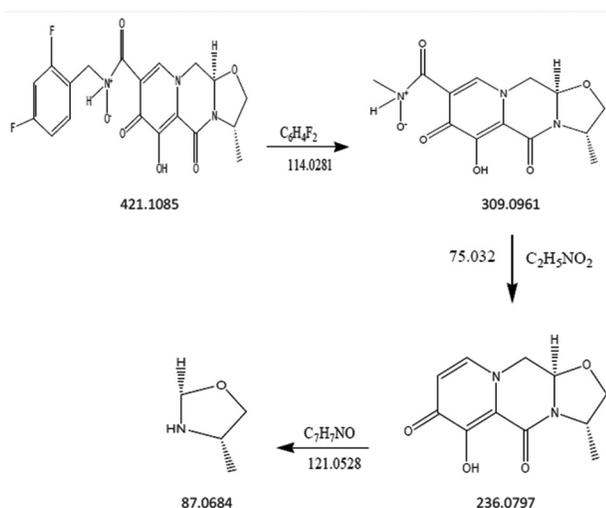
**Figure 19:** Mass fragmentation of scheme 7
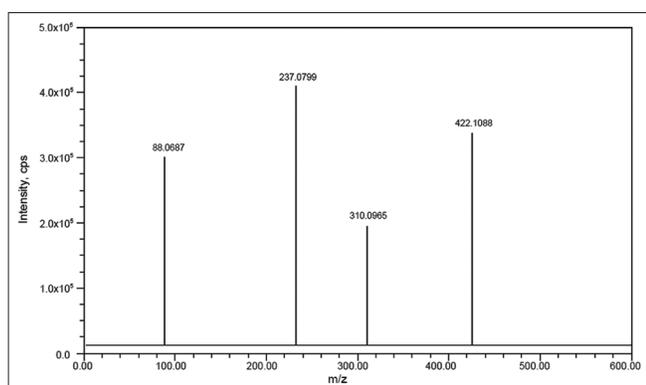
Figure 20: Mass spectra of DP7

REFERENCES

1. Cohen MS, Chen YQ, McCauley M, Gamble T, Hosseinipour MC, Kumarasamy N, *et al*. Antiretroviral therapy for the prevention of HIV-1 transmission. N Engl J Med 2016;375:830-9.
2. Aves T, Tambe J, Siemieniuk RA, Mbuagbaw L. Antiretroviral resistance testing in HIV-positive people. Cochrane Database Syst Rev 2018;11:CD006495.
3. Owens DK, Davidson KW, Krist AH, Barry MJ, Cabana M, Caughey AB, *et al*. Preexposure prophylaxis for the prevention of HIV infection. JAMA 2019;321:2203-13.
4. Liu JP, Manheimer E, Yang M. Herbal medicines for treating HIV infection and AIDS. Cochrane Database Syst Rev 2005;3:CD003937.
5. Zeyrek AS, Takmak Ş, Kurban NK, Arslan S. Systematic review and meta-analysis: Physical-procedural interventions used to reduce pain during intramuscular injections in adults. J Adv Nurs 2019;75:3346-61.
6. Giovanetti M, Ciccozzi M, Parolin C, Borsetti A. Molecular epidemiology of HIV-1 in African countries: A comprehensive overview. Pathogens 2020;9:1072.
7. Sallam M, Şahin GÖ, Ingman M, Widell A, Esbjörnsson J, Medstrand P. Genetic characterization of human immunodeficiency virus Type 1 transmission in the Middle East and North Africa. Heliyon 2017;3:e00352.
8. De Clercq E. The role of non-nucleoside reverse transcriptase inhibitors (NNRTIs) in the therapy of HIV-1 infection. Antiviral Res 1998;38:153-79.
9. Ayuso-Mateos JL, Vázquez-Barquero JL, Dowrick C, Lehtinen V, Dalgard OS, Casey P, *et al*. Depressive disorders in Europe: Prevalence figures from the ODIN study. Br J Psychiatry 2001;179:308-16.
10. Choi SW, Schalet B, Cook KF, Cella D. Establishing a common metric for depressive symptoms: Linking the BDI-II, CES-D, and PHQ-9 to PROMIS depression. Psychol Assess 2014;26:513-27.
11. Banno M, Tsujimoto Y, Kohmura K, Dohi E, Taito S, Someko H, *et al.* Unclear insomnia concept in randomized controlled trials and systematic reviews: A meta-epidemiological study. Int J Environ Res Public Health 2022;19:12261.
12. Van Straten A, van der Zweerde T, Kleiboer A, Cuijpers P, Morin CM, Lancee J. Cognitive and behavioral therapies in the treatment of insomnia: A meta-analysis. Sleep Med Rev 2018;38:3-16.
13. Shapiro ED. Clinical practice. Lyme disease. N Engl J Med 2014;370:1724-31.
14. Stellbrink HJ. Antiviral drugs in the treatment of AIDS: What is in the pipeline? Eur J Med Res 2007;12:483-95.
15. Goebel F, Yakovlev A, Pozniak AL, Vinogradova E, Boogaerts G, Hoetelmans R, *et al*. Short-term antiviral activity of TMC278--a novel NNRTI--in treatment-naive HIV-1-infected subjects. AIDS 2006;20:1721-6.
16. Ashour ML, Youssef FS, Gad HA, Wink M. Inhibition

of cytochrome P450 (CYP3A4) activity by extracts from 57 plants used in traditional Chinese medicine (TCM). Pharmacogn Mag 2017;13:300-8.

17. Vetrichelvan O, Gorjala P, Goodman O Jr, Mitra R. Bergamottin a CYP3A inhibitor found in grapefruit juice inhibits prostate cancer cell growth by downregulating androgen receptor signaling and promoting G0/G1 cell cycle block and apoptosis. PLoS One 2021;16:e0257984.

18. Nevitt SJ, Marson AG, Smith CT. Carbamazepine versus phenytoin monotherapy for epilepsy: An individual participant data review. Cochrane Database Syst Rev 2019;7:CD001911.

19. Rissardo JP, Caprara AL. Phenytoin psychosis. Apollo Med 2020;17:295-6.

20. Barbarino JM, Haidar CE, Klein TE, Altman RB. PharmGKB summary: Very important pharmacogene information for UGT1A1. Pharmacogenet Genomics 2014;24:177-83.

21. AlFadhli S, Al-Jafer H, Hadi M, Al-Mutairi M, Nizam R. The effect of UGT1A1 promoter polymorphism in the development of hyperbilirubinemia and cholelithiasis in hemoglobinopathy patients. PLoS One 2013;8:e77681.

22. Yang M, He Q, Gao F, Nirantharakumar K, Veenith T, Qin X, *et al*. Regular use of proton-pump inhibitors and risk of stroke: A population-based cohort study and meta-analysis of randomized-controlled trials. BMC Med 2021;19:316.

23. Singh A, Hussain S, Jha R, Jayraj AS, Klugar M and Antony B. Proton pump inhibitor use and the risk of hepatocellular carcinoma: A systematic review of pharmacoepidemiological data. J Evid Based Med 2021;14:278-80.